Science Advances
AAAS

advances.sciencemag.org/cgi/content/full/6/32/eaba2423/DC1

Supplementary Materials for

When floods hit the road: Resilience to flood-related traffic disruption in the San Francisco Bay Area and beyond

Indraneel G. Kasmalkar, Katherine A. Serafin, Yufei Miao, I. Avery Bick, Leonard Ortolano, Derek Ouyang, Jenny Suckale*

*Corresponding author. Email: jsuckale@stanford.edu

Published 5 August 2020, *Sci. Adv.* **6**, eaba2423 (2020)
DOI: 10.1126/sciadv.aba2423

This PDF file includes:

Additional Details on Adapting to Rising Tides flood maps

The Adapting to Rising Tides (ART) flood maps used in our model are 1-meter resolution maps, designed specifically to aid sea level rise adaptation planning efforts in the San Francisco Bay Area (*6*). These maps were derived from outputs of the regional hydrodynamic model used during the Federal Emergency Management Agency (FEMA) San Francisco Bay Area coastal study. The FEMA model included over 30 years of hindcasted water levels in 15-minute increments for 900 points around the San Francisco Bay (*40*). The flood maps take a "response-based" statistical approach to define recurrence intervals for extreme water levels based on the historical conditions modeled. This approach derives the magnitude of an extreme water level by incorporating potential combinations of storm surges, tides, seasonal cycles, interannual anomalies driven by large-scale climate variability such as the El Niño Southern Oscillation, and sea level rise. Present-day sea level is defined in the ART flood maps as the mean higher high water (MHHW) over the period 1983 – 2001 which corresponds to the National Oceanic and Atmospheric Administration's current National Tidal Datum.

During the ART flood modeling process, the water surface at the coastline is extended over an inland topography bare-earth digital elevation model with a 1-meter resolution (*6*). While this flood mapping approach does not include the physics of overland flow, the hydraulic connectivity of each flood map raster grid cell is assessed using an "eight-side rule" for connectedness, where each grid cell is considered "connected" if any of its cardinal or diagonal directions is connected to a flooded grid cell (*41*). The hydraulic connectivity removes areas from the areas of inundation that are low-lying but not directly connected to adjacent inundated areas and/or that are protected by levees or other features that prevent inland flooding (*6*). Readers interested in specific details of the ART flood maps should refer to (*6*, *40*) for a complete documentation of methodologies.

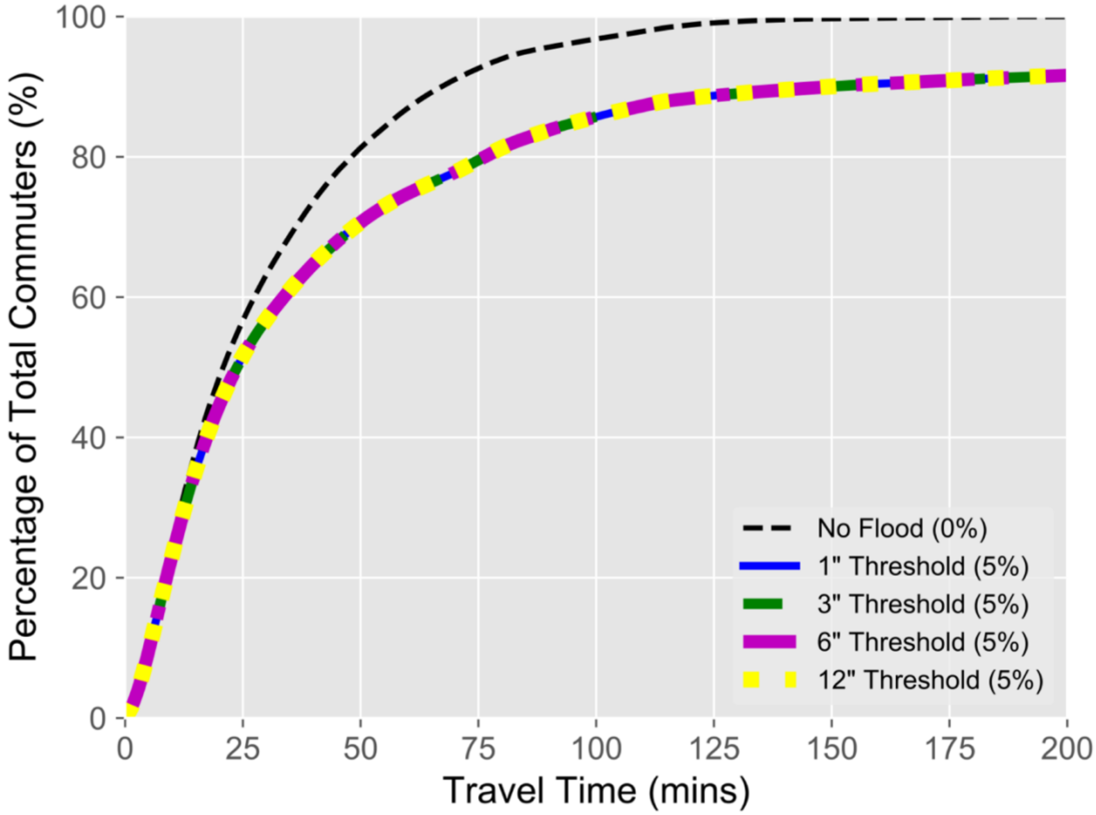

Fig. S1. Cumulative distribution of percentage of commuters over travel time for the 36" water level under various thresholds of road closures. For example, the 1" Threshold simulation closes road segments with at least 1" of inundation, and with 17% of its length covered by water (see the Model section). This latter condition of at least 17% water-cover causes the model to be highly insensitive to the threshold of inundation for thresholds under 12". The percentage of commuters with impassable commutes for each threshold is given in parentheses within the legend.

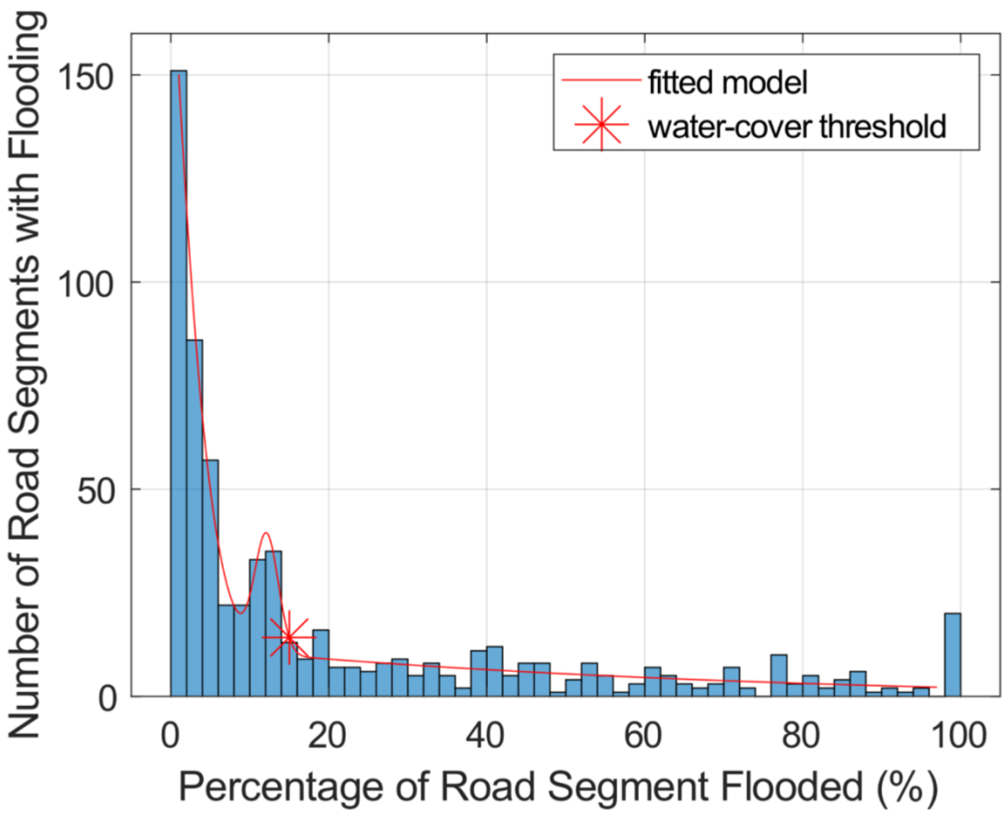

Fig. S2. Histogram over all road segments of the percentage of road length covered by water, for the 36" water level. The histogram indicates three peaks, one at 0% flooded, one at 100% flooded, and one between 12% and 20% flooded. We identify these peaks using a peak-fitted Gaussian Model, shown as a red curve. We derive the water-cover threshold as the inflection point between the second and third peak, and average over all water levels.

Table S1. Various combinations of extreme water level events and sea level rise depicted in the water levels. The water levels considered in this study include present-day sea level, and up to 6” of sea level rise.

Water level	Combinations of extreme water level events and sea level rise	
12”	1-yr extreme water level over present-day sea level	
24”	5-yr extreme water level over present-day sea level	2-yr extreme water level over 6” sea level rise
36”	50-yr extreme water level over present-day sea level	20-yr extreme water level over 6” sea level rise

Table S2: Proportion of employees living and working in the sub-regions of the San Francisco Bay Area. This table is derived from the LODES dataset (*18*). The North Bay region consists of Marin, Napa, Sonoma, and Solano Counties. The East Bay region consists of Alameda and Contra Costa Counties. The South Bay and Peninsula region consists of Santa Clara, San Francisco and San Mateo Counties.

Region of Residence	Proportion of Employees Who Live in Region of Residence and Work in:		
	North Bay	**East Bay**	**South Bay and Peninsula**
North Bay	69%	14%	17%
East Bay	4%	63%	33%
South Bay and Peninsula	2%	11%	87%

Table S3. County-averaged data of flooded road capacity, metric reach, impassability, and travel-time delays.

County	Average Metric Reach (miles)	Flooded Road Capacity (%)			Percentage of Impassable Commutes for County Workplaces (%)			Average Travel-Time Delays (minutes/mile)		
		12”	24”	36”	12”	24”	36”	12”	24”	36”

Alameda	50	0.1	0.2	1.0	0.1	0.2	3	0.01	0.01	0.02
Contra Costa	45	0.3	0.4	0.4	0.1	0.3	0.6	0.02	0.02	0.01
Marin	26	7.0	11.5	14.5	14	18	24	0.9	0.9	1.2
Napa	28	0.7	0.7	1.0	0.2	0.4	0.6	0.1	0.1	0.4
San Francisco	56	0.08	0.08	0.1	0.4	0.6	2	0.0008	0.0008	0.001
San Mateo	43	0.4	2.0	7.1	3	4	13	0.0001	0.004	0.02
Santa Clara	52	0.01	0.4	1.8	0.05	0.9	6	0.0001	0.006	0.02
Solano	34	0.5	1.2	1.6	0.3	1	1	0.03	0.03	0.03
Sonoma	32	0.4	0.3	0.5	0.2	0.5	2	0.2	0.2	0.2

Table S4. Linear regression with log-transformed data of average travel-time delays versus average metric reach and percentage of road capacity flooded for the 36" water level. Regression performed over the nine counties of the San Francisco Bay Area. Data provided in Table S3.

Dependent Variable	Log Average Travel-Time Delay per Mile for 36" Water Level			
Model	Ordinary Least Squares Regression			
R-squared	0.863	**F-statistic**	18.96	
Adj. R-squared	0.818	**Prob (F-statistic)**	0.00255	
Condition Number	89.7	**Log-Likelihood**	-10.094	
Independent Variables	**Coefficients**	**Standard Error**	**t-score**	**p-value (P > |t|)**
constant	21.1396	4.448	4.753	0.003
Log Average Metric Reach	-6.2404	1.323	-4.717	0.003
Log Flooded Capacity	0.3256	0.261	1.245	0.259

Table S5. Linear regression with log-transformed data of average travel-time delays versus average metric reach and percentage of road capacity flooded for the 12" water level. Regression performed over the nine counties of the San Francisco Bay Area. Data provided in Table S3.

Dependent Variable	Log Average Travel-Time Delay per Mile for 12" Water Level			
Model	Ordinary Least Squares Regression			
R-squared	0.796	**F-statistic**	11.74	
Adj. R-squared	0.729	**Prob (F-statistic)**	0.00844	
Condition Number	170	**Log-Likelihood**	-13.749	
Independent Variables	**Coefficients**	**Standard Error**	**t-score**	**p-value (P > |t|)**
constant	24.8272	11.115	2.234	0.067
Log Average Metric Reach	-7.6880	3.726	-2.063	0.085
Log Flooded Capacity	0.1163	0.497	0.234	0.823

Table S6. Linear regression with log-transformed data of average travel-time delays versus average metric reach and percentage of road capacity flooded for the 24” water level. Regression performed over the nine counties of the San Francisco Bay Area. Data provided in Table S3.

Dependent Variable	Log Average Travel-Time Delay per Mile for 24” Water Level			
Model	Ordinary Least Squares Regression			
R-squared	0.856	**F-statistic**	17.85	
Adj. R-squared	0.808	**Prob (F-statistic)**	0.00298	
Condition Number	124	**Log-Likelihood**	-10.582	
Independent Variables	**Coefficients**	**Standard Error**	**t-score**	**p-value (P > |t|)**
constant	22.3527	5.631	3.969	0.007
Log Average Metric Reach	-7.0133	1.775	-3.952	0.008
Log Flooded Capacity	0.0649	0.256	0.254	0.808

REFERENCES AND NOTES

1. S. I. Seneviratne, N. Nicholls, D. Easterling, C. M. Goodness, S. Kanae, J. Kossin, Y. Luo, J. Marenggo, K. McInnes, M. Rahimi, M. Reichstein, A. Sorteberg, C. Vera, X. Zhang, Chapter 3. Changes in Climate Extremes and their Impacts on the Natural Physical Environment, in *Managing the risks of extreme events and disasters to advance climate change adaptation. A Special Report of Working Groups I and II of the Intergovernmental Panel on Climate Change (IPCC*), C. B. Field, V. R. Barros, D. J. Dokken, K. J. Mach, M. D. Mastrandrea, T. E. Bilir, M. Chatterjee, K. L. Ebi, Y. O. Estrada, R. C. Genova, B. Girma, E. S. Kissel, A. N. Levy, S. MacCracken, P. R. Mastrandrea, L. L. White, Eds. (Cambridge Univ. Press, 2012), pp. 109–230.

2. P. P. Wong, I. J. Losada, J. P. Gattuso, J. Hinkel, A. Khattabi, K. L. McInnes, Y. Saito, A. Sallenger, Chapter 5. Coastal systems and low-lying areas, in *Climate Change 2014: Impacts, Adaption and Vulnerability. Part A: Global and Sectoral Aspects. Contribution of Working Group II to the Fifth Assessment Report of the Intergovernmental Panel on Climate Change*, C. B. Field, V. R. Barros, D. J. Dokken, K. J. Mach, M. D. Mastrandrea, T. E. Bilir, M. Chatterjee, K. L. Ebi, Y. O. Estrada, R. C. Genova, B. Girma, E. S. Kissel, A. N. Levy, S. MacCracken, P. R. Mastrandrea, L. L. White, Eds. (Cambridge Univ. Press, 2014), pp. 361–409.

3. A. Revi, D. E. Satterthwaite, F. Aragón-Durand, J. Corfee-Morlot, R. B. R. Kiunsi, M. Pelling, D. C. Roberts, W. Solecki, Chapter 8. Urban Areas, in *Climate Change 2014: Impacts, Adaptation, and Vulnerability. Part A: Global and Sectoral Aspects. Contribution of Working Group II to the Fifth Assessment Report of the Intergovernmental Panel on Climate Change*, C. B. Field, V. R. Barros, D. J. Dokken, K. J. Mach, M. D. Mastrandrea, T. E. Bilir, M. Chatterjee, K. L. Ebi, Y. O. Estrada, R. C. Genova, B. Girma, E. S. Kissel, A. N. Levy, S. MacCracken, P. R. Mastrandrea, L. L. White, Eds. (Cambridge Univ. Press, 2014), pp. 535–612.

4. United Nations Population Division, "World Urbanization Prospects: The 2018 Revision" (2018).

5. M. Oppenheimer, M. Campos, R. Warren, J. Birkmann, G. Luber, B. O'Neill, K. Takahashi, Chapter 19. Emergent Risks and Key Vulnerabilities, in *Climate Change 2014: Impacts, Adaptation, and Vulnerability. Part A: Global and Sectoral Aspects. Contribution of Working Group II to the Fifth Assessment Report of the Intergovernmental Panel on Climate Change*, C. B. Field, V. R. Barros, D.

J. Dokken, K. J. Mach, M. D. Mastrandrea, T. E. Bilir, M. Chatterjee, K. L. Ebi, Y. O. Estrada, R. C. Genova, B. Girma, E. S. Kissel, A. N. Levy, S. MacCracken, P. R. Mastrandrea, L. L. White, Eds. (Cambridge Univ. Press, 2014), pp. 1039–1099.

6. J. Vandever, M. Lightner, S. Kassem, J. Guyenet, M. Mak, C. Bonham-Carter, Adapting to Rising Tides Bay Area Sea Level Rise Analysis and Mapping Project (2017); www.adaptingtorisingtides.org/wp-content/uploads/2018/07/BATA-ART-SLR-Analysis-and-Mapping-Report-Final-20170908.pdf.

7. B. S. Kerner, *The Physics of Traffic: Empirical Freeway Pattern Features, Engineering Applications, and Theory* (Springer, 2012).

8. D. Freckleton, K. Heaslip, W. Louisell, J. Collura, Evaluation of resiliency of transportation networks after disasters. *Transp. Res. Rec.* **2284**, 109–116 (2012).

9. A. A. Ganin, M. Kitsak, D. Marchese, J. M. Keisler, T. Seager, I. Linkov, Resilience and efficiency in transportation networks. *Sci. Adv.* **3**, e1701079 (2017).

10. L.-G. Mattsson, E. Jenelius, Vulnerability and resilience of transport systems—A discussion of recent research. *Transp. Res. Part A Policy Pract.* **81**, 16–34 (2015).

11. E. Jenelius, Redundancy importance: Links as rerouting alternatives during road network disruptions. *Procedia Eng.* **3**, 129–137 (2010).

12. X. Xu, A. Chen, S. Jansuwan, K. Heaslip, C. Yang, Modeling transportation network redundancy. *Transp. Res. Procedia* **9**, 283–302 (2015).

13. H. Demirel, M. Kompil, F. Nemry, A framework to analyze the vulnerability of European road networks due to sea-level rise (SLR) and sea storm surges. *Transp. Res. Part A Policy Pract.* **81**, 62–76 (2015).

14. A. Reggiani, P. Nijkamp, D. Lanzi, Transport resilience and vulnerability: The role of connectivity. *Transp. Res. Part A Policy Pract.* **81**, 4–15 (2015).

15. S. Weilant, A. Strong, B. M. Miller, *Incorporating Resilience into Transportation Planning and Assessment* (RAND Corporation, 2019).

16. S. A. Markolf, C. Hoehne, A. Fraser, M. V. Chester, B. S. Underwood, Transportation resilience to climate change and extreme weather events – Beyond risk and robustness. *Transp Policy* **74**, 174–186 (2019).

17. A. Pisarski, *Commuting in America III: The Third National Report on Commuting Patterns and Trends* (Transportation Research Board, 2006), vol. 550.

18. United States Census Bureau, Longitudinal Employer-Household Dynamics Origin Destination Employment Statistics—Geodatabase Format: 2015 (2015); https://lehd.ces.census.gov/data/.

19. P. Suarez, W. Anderson, V. Mahal, T. R. Lakshmanan, Impacts of flooding and climate change on urban transportation: A systemwide performance assessment of the Boston Metro Area. *Transp. Res. D Transp. Environ.* **10**, 231–244 (2005).

20. P. Wang, T. Hunter, A. M. Bayen, K. Schechtner, M. C. González, Understanding road usage patterns in urban areas. *Sci. Rep.* **2**, 1001 (2012).

21. M. Chen, A. S. Alfa, A network design algorithm using a stochastic incremental traffic assignment approach. *Transp. Sci.* **25**, 215–224 (1991).

22. Metropolitan Transportation Commission/Association of Bay Area Governments (MTC/ABAG), Regional Road Network—Shapefile Format: 2015 (2017); http://analytics.mtc.ca.gov/foswiki/bin/view/Main/DataRepository.

23. G. Erhardt, D. Ory, A. Sarvepalli, J. Freedman, J. Hood, B. Stabler, MTC's Travel Model One: Applications of an Activity-Based Model in its First Year, paper presented at the *5th Transportation Research Board Innovations in Travel Modeling Conference, Tampa, Florida*. Originally presented at and winner of Best Presentation award at Futura 2011: Citilabs Annual International Users Conference, Palm Springs, CA, (2012).

24. United States Census Bureau, American Community 1-Year Survey—Geodatabase Format: 2016 (2016).

25. United States Census Bureau, TIGER/Line Shapefile Products—Shapefile Format: 2018 (2015); www.census.gov/geographies/mapping-files/time-series/geo/tiger-line-file.html.

26. National Research Council, *Sea-Level Rise for the Coasts of California, Oregon, and Washington: Past, Present, and Future* (The National Academis Press, 2012).

27. California Natural Resources Agency, California Ocean Protection Council, State of California Rise Guidance—2018 Update (2018); www.opc.ca.gov/updating-californias-sea-level-rise-guidance/.

28. National Oceanic and Atmospheric Administration, Turn Around Don't Drown, *National Weather Service*; www.weather.gov/safety/flood-turn-around-dont-drown.

29. M. Pregnolato, A. Ford, S. M. Wilkinson, R. J. Dawson, The impact of flooding on road transport: A depth-disruption function. *Transp. Res. D Transp Environ.* **55**, 67–81 (2017).

30. California Department of Transportation (Caltrans), California Road Elevation Measurement—Shapefile Format: 2016 (2016).

31. D. J. Tyler, Topobathymetric Model for the San Francisco Bay, California, 1929 to 2017: U.S. Geological Survey Data Release (2018); https://doi.org/10.5066/F7736Q34.

32. J. Suh, A. T. Siwe, S. M. Madanat, Transportation infrastructure protection planning against sea level rise: Analysis using operational landscape units. *J. Infrastruct. Syst.* **25**, 04019024 (2019).

33. A. Colsaet, Y. Laurans, H. Levrel, What drives land take and urban land expansion? A systematic review. *Land Use Policy* **79**, 339–349 (2018).

34. C. Benner, A. Karner, Low-wage jobs-housing fit: Identifying locations of affordable housing shortages. *Urban Geogr.* **37**, 883–903 (2016).

35. A. Mann, T. Luo, Crash and reboot: Silicon Valley high-tech employment and wages, 2000–08. *Mon. Labor Rev.* **141**, 59–73 (2010).

36. Metropolitan Transportation Commission, Association of Bay Area Governments, Plan Bay Area 2040 (2017); http://2040.planbayarea.org/reports.

37. P. Crucitti, V. Latora, S. Porta, Centrality measures in spatial networks of urban streets. *Phys. Rev. E.* **73**, 036125 (2006).

38. A. Kermanshah, S. Derrible, Robustness of road systems to extreme flooding: Using elements of GIS, travel demand, and network science. *Nat. Hazards* **86**, 151–164 (2017).

39. J. Peponis, S. Bafna, Z. Zhang, The connectivity of streets: Reach and directional distance. *Environ. Plann. B Plann. Des.* **35**, 881–901 (2008).

40. M. Mak, E. Harris, M. Lightner, J. Vandever, K. May, *San Francisco Bay Tidal Datums and Extreme Tides Study*, Prepared for the Federal Emergency Management Agency by AECOM: Oakland, CA, USA (2016); https://www.adaptingtorisingtides.org/wp-content/uploads/2016/05/20160429.SFBay_Tidal-Datums_and_Extreme_Tides_Study.FINAL_.pdf.

41. D. Marcy, B. William, K. Dragonoz, B. Hadley, C. Haynes, N. Herold, J. McCombs, M. Pendleton, S. Ryan, K. Schmid, M. Sutherland, K. Waters, New Mapping Tool and Techniques or Visualizing Sea Level Rise and Coastal Flooding Impacts, in *Proceedings of the 2011 Solutions to Coastal Disasters Conference*, Anchorage, AK, June 2011.